Title: Temporal pattern and synergy influence activity of ERK signaling pathways during L-LTP induction

Authors:

1. Nadiatou Miningou
   Department of Chemistry and Biochemistry, George Mason University, Fairfax, VA 22030
2. Kim T. Blackwell
   Interdisciplinary Program in Neuroscience, Bioengineering Department, and Krasnow Institute for Advanced Study, George Mason University, Fairfax, VA 22030

Corresponding Author: Kim T. Blackwell, Krasnow Institute for Advance Study, MS 2A1, George Mason University, 4400 University Drive, Fairfax, VA, 22030,

Conflict of Interest: The authors declare no competing financial interests.

Acknowledgements: This work was supported through the joint NIH-NSF CRCNS program through NSF grant 1515686 and NIMH grant R01MH 117964

Competing interests: The authors declare no competing interests

ABSTRACT

Long lasting long-term potentiation (L-LTP) is a cellular mechanism of learning and memory storage. Studies have demonstrated a requirement for the extracellular signal-regulated kinase (ERK) activation in L-LTP produced by a diversity of temporal stimulation patterns. Multiple signaling pathways converge to activate ERK, with different pathways being required for different stimulation patterns. We addressed the critical questions of whether maximal activation of ERK requires multiple pathways, and whether different temporal patterns select different signaling pathways for ERK activation. We developed a computational model of five signaling pathways (including two novel pathways) leading to ERK activation during L-LTP. Simulations show that calcium and cAMP work synergistically to activate ERK, and that stimuli given with large inter-trial intervals activate more ERK than shorter intervals, a temporal sensitivity similar to PKA but contrary to CaMKII. These results suggest that signaling pathways with different temporal sensitivity facilitate ERK activation to diversity of temporal patterns.

INTRODUCTION

Long-term potentiation (LTP), the activity-dependent and persistent strengthening of synapses, is widely considered to be a cellular mechanism underlying memory storage. Late phase LTP (L-LTP), induced by repetitive stimulation, lasts over 8 hours and involves de novo protein synthesis (Davis et al., 2000; Sweatt, 2004; Tang and Yasuda, 2017). Another critical molecule in synaptic plasticity and memory is extracelluar signal-regulated kinase (ERK) (English and Sweatt, 1997), as inhibition of ERK inhibits both hippocampal LTP and memory. Numerous studies have demonstrated that ERK contributes to synaptic plasticity by controlling transcription and protein translation (for review Miningou and Blackwell, 2020; Peng et al., 2010), as well as increasing cell excitability by phosphorylating potassium channels (Schrader et al., 2006).

ERK is a serine-threonine protein kinase activated upon dual phosphorylation by Mitogen-activated kinase kinase (MEK), which is in turn dually phosphorylated and activated by Raf family kinases (Buscà et al., 2016; Terrell and Morrison, 2019). Raf kinases are activated by Ras family GTP binding proteins, Rap1 and Ras, which are controlled by Guanine nucleotide Exchange Factors (GEFs) and GTPase Activating Proteins (GAPs) that activate (via the

exchange of bound GDP for GTP) or inactivate (via hydrolysis of GTP to GDP) them, respectively.

In the hippocampus, the ERK cascade is initiated through several pathways. Influx of the second messenger calcium, through the NMDA receptor, activates the calcium-sensitive GEF RasGRF and inhibits SynGap, the synaptically localized GAP, by CaMKII phosphorylation. In the hippocampus, calcium or the GαsGTP subunits of the active β-adrenergic receptors (βARs) activate the intracellular second messenger Cyclic Adenosine MonoPhosphate (cAMP), which activates two key molecules upstream of ERK activation: protein kinase A (PKA) and the GEF exchange factor activated by cAMP (Epac)(de Rooij et al., 2000; Enserink et al., 2002; Schmitt and Stork, 2002). cAMP binding to Epac exposes the Rap-binding site allowing the exchange of Rap1GDP to Rap1GTP. Once activated, PKA phosphorylates the kinase Src, which through multiple steps activates Rap1GTP, or phosphorylates βARs, causing βγ subunits of Gi (Giβγ) to recruit Src leading to RasGTP production (Schmitt and Stork, 2002).

Given the importance of ERK signaling pathway in LTP, several models of ERK (Ajay and Bhalla, 2004; Jain and Bhalla, 2014; Neves et al., 2008) have investigated how negative feedback loops, feedforward loops, spatial pattern or temporal pattern controls the dynamics of ERK. These models demonstrated a role for PKC or PKA in ERK activation, but they did not consider the role of SynGap or Epac, which are critical for some forms of L-LTP (Araki et al., 2020; Gelinas et al., 2008; Komiyama et al., 2002; Rumbaugh et al., 2006). Furthermore, key ERK activators, such as PKA and CaMKII, exhibit different temporal sensitivity: cAMP/PKA favors spaced LTP stimulation protocols (Kim et al., 2010; Scharf et al., 2002; Woo et al., 2003) while calcium/CaMKII prefers massed LTP stimulation (Ajay and Bhalla, 2004; Kim et al., 2010). A critical question is how patterns of synaptic input determine which set of signaling pathways activate ERK leading to the induction of L-LTP. A second critical question is whether those signaling pathways work synergistically to activate ERK. To investigate these questions, we developed a single compartment computational biochemical model of postsynaptic signaling pathway underlying L-LTP in hippocampal CA1 pyramidal neurons. Simulations reveal that ERK pathways work synergistically and show that the contribution of cAMP increases while the calcium contribution decreases with space stimuli.

RESULTS

Single-pulse stimuli: maximal ERK activation requires multiple pathways

To investigate how temporal pattern of synaptic activity determines which pathway in the ERK signaling cascade (Figure 1A) dominates in dendritic spines of hippocampal CA1 pyramidal neurons, we developed a single compartment, stochastic reaction-diffusion model of pathways activating ERK. The model included two calcium signaling pathways (RasGRF and SynGap) and three cAMP signaling pathways (Epac, PKA and the βγ subunit of Gi). In order to assess if multiple pathways are required for maximal ERK activation, both single pathway and multi-pathway dynamics were monitored. Simulation experiments used different amplitude ranges (for 1 sec) and different durations of the input to evaluate doubly phosphorylated ERK (ppERK) (Table 1). Characteristics assessed included whether the ERK response is graded versus ultra-sensitive and whether the response to a combination of some pathways exhibited a nonlinear response.

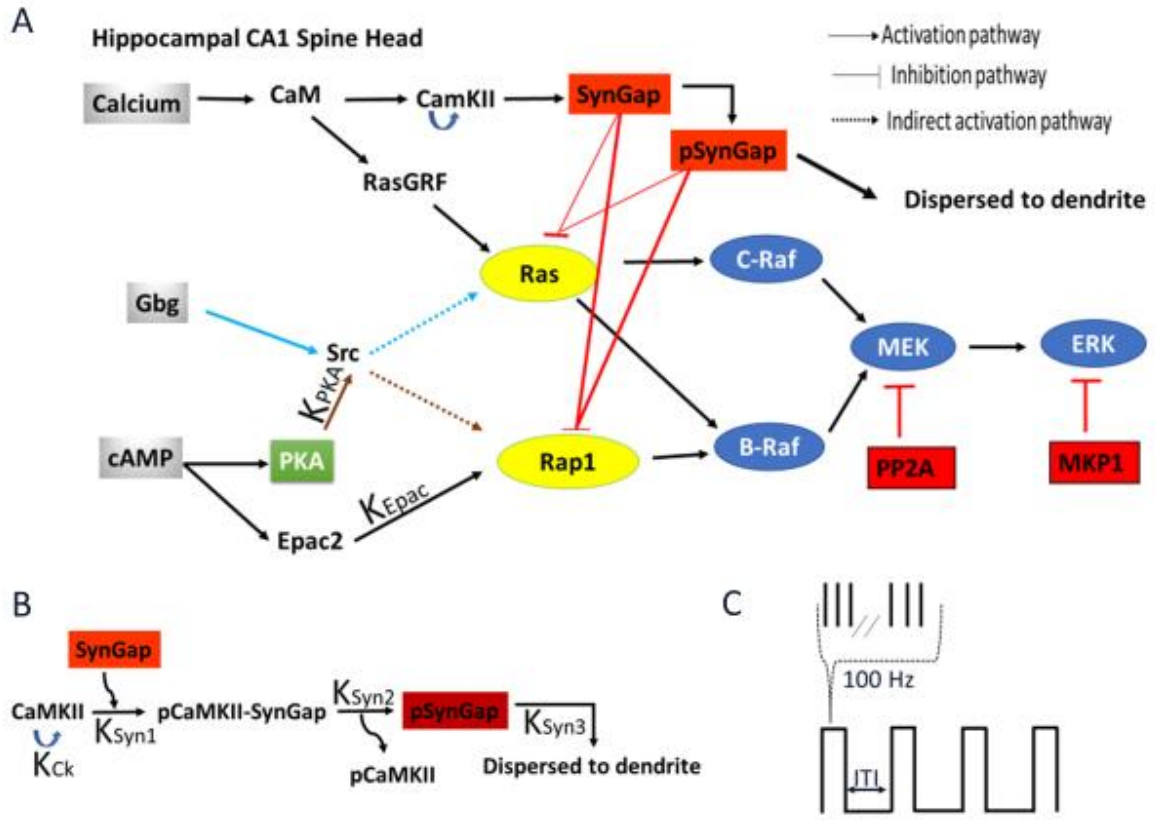

Figure 1: ***A. Schematic representation of signaling pathways activating ERK. Five pathways are included in the model:*** *calcium activation of (1) RasGRF followed by RasGTP production or (2) CaMKII modulation of SynGap followed by increasing RasGTP and Rap1GTP lifetime; cAMP activation of (3) Epac or (4) PKA phosphorylation of Src family kinase, leading to Rap1GTP production; Gi subtype of GTP binding protein (Giβγ) (5) recruits Src family kinase followed by activation of RasGTP.* ***B.*** *Three effects of CaMKII on SynGap were evaluated:* K_{Syn1}*. No SynGap bound,* K_{Syn2}*. SynGap bound (but not phosphorylated),* K_{Syn3}*. SynGap phosphorylated, but not dispersed to dendrite.* ***C. LTP protocol****: four trains of 100 Hz (each 1 sec duration) spaced by different intertrial interval: 3, 20, 40, 80 and 300 sec.*

Table 1: ***Single pathway experiment***

Input	Amplitude protocol (μM)	Duration protocol (sec)
Calcium	1 sec: 0.2, 0.3, 0.5,1,1.5,2,5	0.5 μM: 1,2,4, 5,6, 8,10,30,100 1 μM: 1,4, 100
cAMP	1 sec: 0.1,0.2,0.5,1,1.5,2	0.1 μM: 1,4,10,30,100 0.5 μM: 1,4,10,30,100
Giβγ	1 sec: 0.005,0.03, 0.1,0.5	0.03 μM: 1,4,10,30,100 0.1 μM: 1,4,10,30,100

Linear activation by cAMP pathway

cAMP activates ERK through three different pathways: Epac activation of Rap1GTP, PKA phosphorylation of Src and PKA phosphorylation of βAR, which switches βAR from Gs coupling to Gi coupling, followed by Giβγ recruitment of Src. To separate the direct action of cAMP from its action through the switching pathway, we evaluated the effect of Giβγ separately and in combination with Epac and PKA direct activation.

Model simulations show a linear activation with either cAMP duration or concentration (Figure 2). As observed in Figure 2A, as the input duration increases, ppERK amplitude and duration increases. However, with cAMP durations of 30 sec or more, ppERK amplitude reaches a plateau, though the duration of ppERK continues to increase. In summary, in response to cAMP input, ppERK total activity is linearly related to the input duration until saturation where it plateaus (Figure 2B).

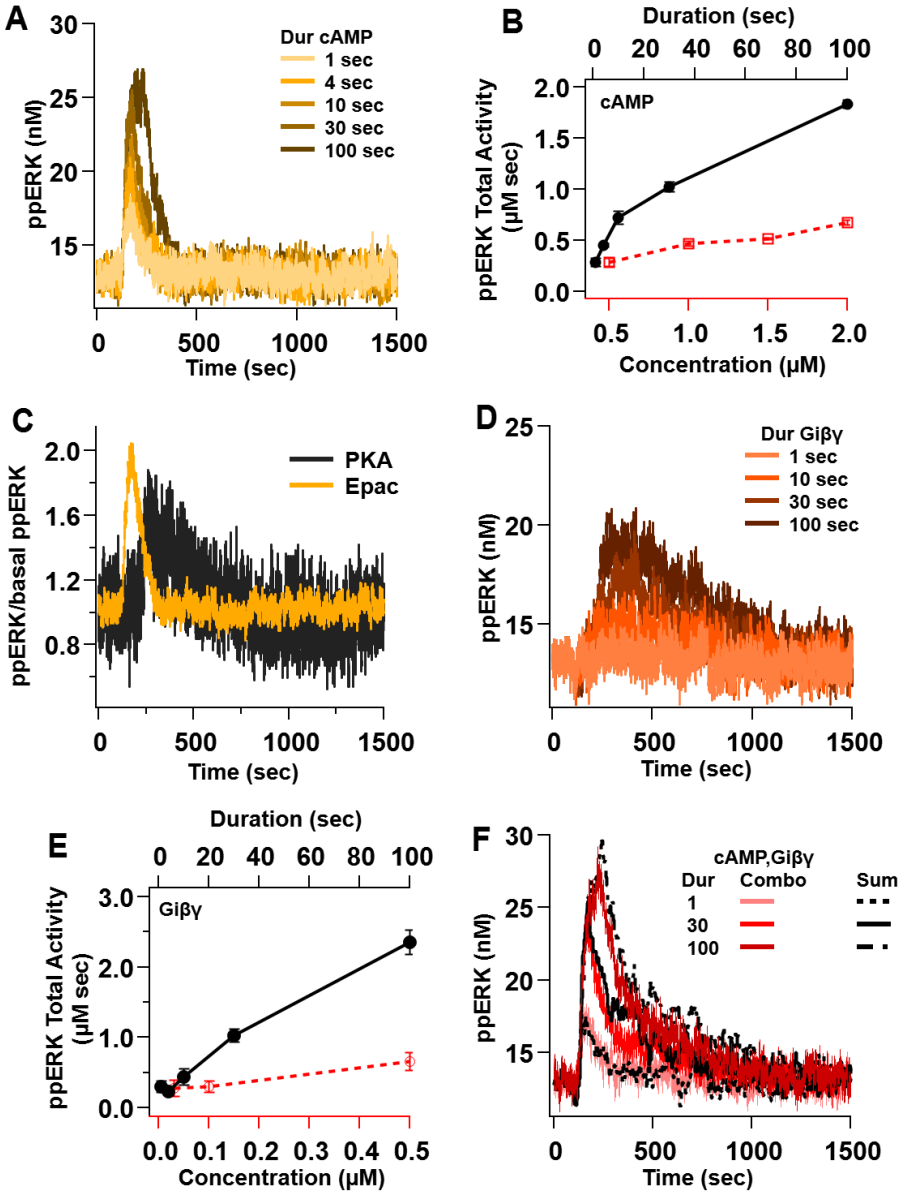

Figure 2: ***Linear activation of ERK by cAMP pathways. A.*** *ppERK response to a single pulse of 0.5 μM cAMP is graded with duration.* ***B.*** *Integral of ppERK concentration over time (AUC) in response to different cAMP concentrations (1 sec) and different cAMP durations (0.5 μM). ppERK activation is more sensitive to cAMP duration than amplitude.* ***C.*** *ppERK increases quickly with Epac and with a delay in response to PKA. Both increase to a similar extent.* ***D.*** *Time course of ppERK in response to single pulses of 0.1 μM Giβγ for different durations. Recruitment of ERK by Giβγ binding protein shows delayed activation.* ***E****. Total activity of ppERK in response to different Giβγ concentrations (1 sec) and durations (0.1 μM). ppERK activation is more sensitive to duration than amplitude.* ***F****. Direct and indirect cAMP pathways combine linearly for all duration inputs and sub-linearly with prolonged duration inputs. Combo: response to Giβγ and cAMP, sum: sum of the responses in A and D.*

To investigate the activation of ERK by Epac and PKA individually, the simulations were repeated with cAMP binding to one of these molecules blocked (Table 2). When cAMP binding to Epac is blocked, the basal quantity of ppERK is dramatically reduced, implying that Epac is the main source of basal ppERK. The remaining activity, due to PKA, shows a delayed activation of ERK with ~1.5 fold change (Figure 2C). Contrary to PKA, Epac produces a fast and transient activation of ERK with slightly more than a 2 fold change (Figure 2C). Thus, both PKA and Epac contribute to ERK activation with different dynamics.

Table 2: ***Knockout experiment****: Rate constant names are shown in Figure 1A, B. Block lists the rate constant whose value is set to zero.*

Input	Block	Effect/Molecular dependence
Calcium 2000 nM for 1 sec	K_{CK}	CaMKII is activated but cannot autophosphorylate itself, thus RasGRF is the only contributor
	K_{Syn1}	pCaMKII is unable to bind to SynGap
	K_{Syn2}	pCaMKII binds to SynGap but unable to release phosphorylated SynGap
	K_{Syn3}	SynGap is phosphorylated but unable to disperse to the dendrite
cAMP 500 nM for 30 sec	K_{Epac}	Epac binds cAMP but cannot activate Rap1GDP, thus PKA is the only contributor
	K_{PKA}	Final step of PKA pathway activation of Rap1GDP is blocked, thus Epac is the only contributor

cAMP also activates ERK through a longer, indirect pathway consisting of PKA phosphorylation of βAR, which switches βAR from Gs to Gi coupling, followed by Giβγ recruitment of Src (Lin et al., 2013; Luttrell et al., 1997). Similarly, to the direct cAMP pathway, the indirect cAMP pathway displays linear activation of ERK with Giβγ input (Figure 2D). However, the activation of ERK is more sensitive to Giβγ duration than concentration (Figure 2E). Similarly to PKA activation, Giβγ produces a delayed activation of ERK consistent with experimental data (Koch et al., 1994; Schmitt and Stork, 2002) and a computational model showing a 7 min delay (Khalilimeybodi et al., 2018). The slow, delayed activation of ERK might explain why the input duration is more effective compared to concentration.

Direct and indirect cAMP pathways combine linearly for short duration inputs and sublinearly with prolonged duration inputs. Figure 3F shows that the response to stimulating all three cAMP pathways overlaps with the sum of the single pathway responses only at a short

duration. As the stimulus duration increases, the ppERK response is slightly lower than the sum of responses to cAMP direct and indirect activation. Sublinear summation is due to two loci of competition. Competition was observed between the PKA phosphorylation of Src and Giβγ activation of Src. Giβγ and PKA showed a delayed activation of ERK, however, PKA has a higher affinity for Src than does Giβγ. Therefore, Src is trapped by PKA, reducing available Src for Giβγ which results in less production of RasGTP compare to Giβγ alone. This sublinear response is observed with 2x and 4x increases in Src quantity (results not shown) demonstrating that the sublinear summation is not due to Src depletion but indeed due to Giβγ and PKA competition with Src. Another competition was observed between Epac and the Giβγ/Crk-C3G for Rap1GDP. Giβγ/ Crk-C3G activation is 86% slower than Epac activation. Therefore, Rap1GDP is consumed by Epac thus reducing available Rap1GDP for Giβγ/Crk-C3G. Blocking Epac allows more Rap1GDP to bind Crk-C3G, prolonging ppERK activity as observed with Giβγ alone. In conclusion, competition between PKA and Giβγ for Src, and between Epac and Crk-C3G for Rap1GDP, affects the summation in cAMP pathway.

Non-linear activation by calcium pathways

Model simulations show a non-linear activation with either calcium duration or concentration. Figure 3A reveals that low calcium inputs produce little to no ppERK, whereas with higher calcium inputs ppERK reaches a plateau and the duration of ppERK is prolonged. Similar results are observed with increasing duration of 0.5 μM calcium concentration. Total activity of ppERK (Figure 3B), reveals a supralinear response (also called ultrasensitivity), with a calcium duration threshold of 4 sec and an amplitude threshold between 1 and 2 μM. A calcium amplitude or duration above these thresholds induces maximal and sustained ppERK.

To determine if the ultrasensitivity of ppERK was caused by CaMKII, we blocked CaMKII phosphorylation (of itself and SynGap) and assessed ERK activation by RasGRF. Blocking CaMKII significantly reduces ppERK activity, especially for long or high calcium inputs. We observed a shift from a sustained and prolonged ppERK to a transient and short ppERK, which is caused by calmodulin activation of RasGRF (Figure 3C). RasGRF activation of ERK is approximately linear and more sensitive to duration than concentration. Thus, similar to the response to cAMP, ERK activation needs time to integrate the signal from RasGRF.

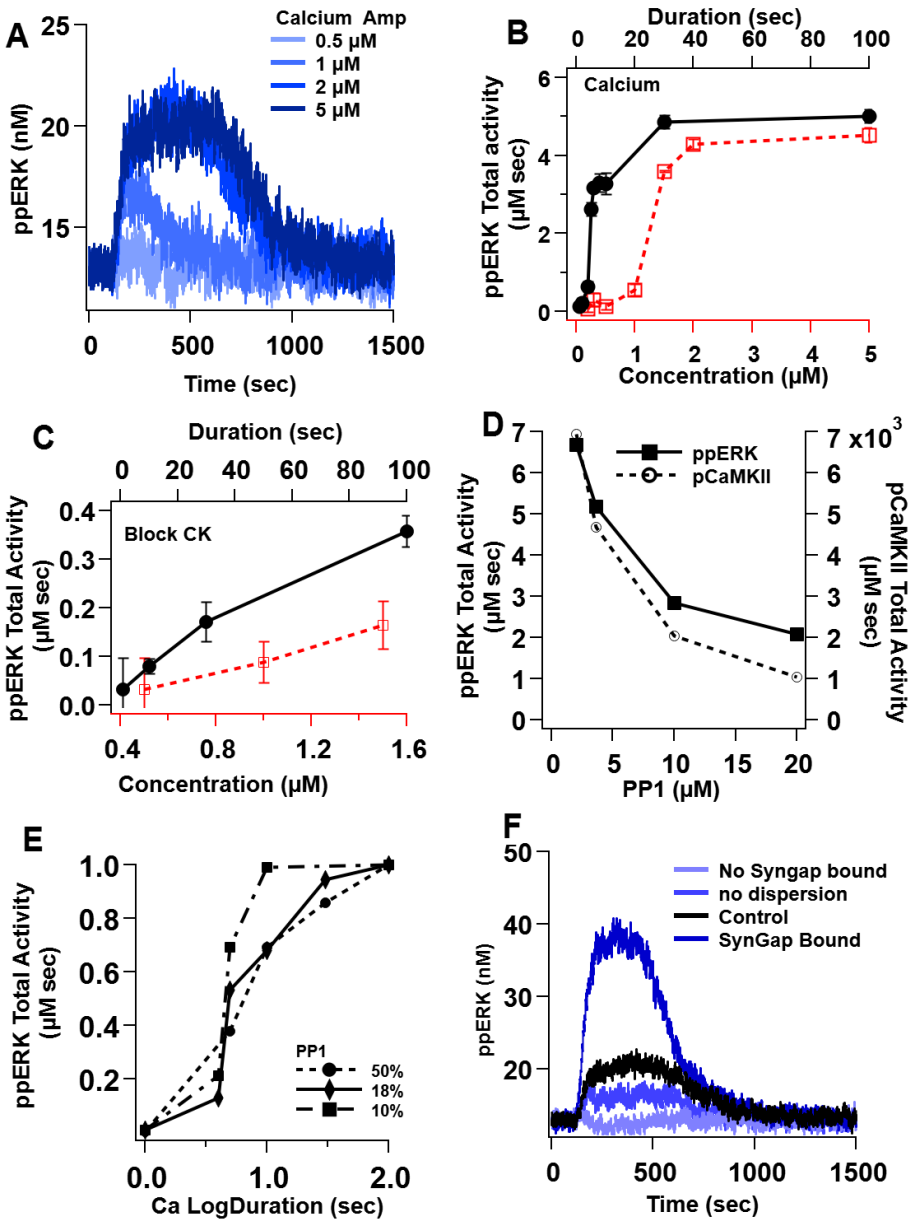

Figure 3: ***Nonlinear activation of ERK by calcium pathway:*** ***A*** *Time course shows a sustained ppERK when calcium is above amplitude threshold (2 µM).* ***B.*** *Total ppERK activity over time in response to different calcium concentrations (1 sec) and different calcium durations (0.5 µM) reveals ultrasensitive response.* ***C.*** *CaMKII activity blocked, changes the system from nonlinear to linear. The remaining RasGRF activation of ppERK is more sensitive to duration than concentration.* ***D.*** *pCaMKII and ppERK activities in response to 0.5 µM for 100 sec of calcium decrease with increase PP1. Similar results were observed with different concentration or duration.* ***E****. Increasing PP1 quantity decreases the steepness of ppERK vs duration (log10) curve.* ***F.*** *Total ERK activity changes with SynGap availability. Blocking dispersion of SynGAP reduces ppERK, whereas allowing CaMKII to bind but not phosphorylate SynGAP enhances ppERK.*

The ultrasensitivity of CaMKII autophosphorylation has been shown to depend on the quantity of the phosphatase PP1 (Bradshaw et al., 2003; Singh and Bhalla, 2018), and thus might regulate the calcium duration and amplitude thresholds. We used a concentration of 3.6 µM of PP1 (PP1: CaMKII ratio = 18%) based on previous reports (Rangamani et al., 2016). To evaluate whether PP1 quantity controls the ppERK non-linear response, we repeated simulations with different quantities of PP1 (10, 50, and 100 % of CaMKII quantity). Model simulations show that CaMKII dynamics are indeed sensitive to PP1 concentration (Figure 3D), regardless of calcium concentration or duration used. The calcium duration producing half maximal ppERK duration did not change much with increase PP1, however both the sensitivity to calcium duration and ppERK amplitude decreased with an increase in PP1 (Figure 3E, Table 3). Thus, our data demonstrate that PP1 indirectly influences ppERK duration and amplitude through modulation of pCaMKII. Therefore, the ultrasensitivity of both CaMKII and ppERK, depends on the ratio of CaMKII to PP1 quantity.

Table 3: ***PP1 concentration influences ppERK quantity and ultrasensitivity.*** *The calcium duration producing half maximal ppERK duration and the sensitivity to duration were estimated by fitting a hill equation to ppERK duration vs calcium duration. Values shown are parameter estimate +/- standard deviation of the estimate. Width at half max represent the calcium duration at half max.*

PP1(%)	Width at half max (sec)	Hill Coefficient
10	4.6 +/- 0.01	9.66 +/- 0.266
18	6.0 +/- 1.9	2.08 +/-1.36
50	5.8 +/- 1.5	1.42 +/- 0.64

CaMKII does not directly activate ERK but instead modulates ERK phosphorylation through its phosphorylation of SynGap, a molecule that inactivates Ras family GTPases. The effect of CaMKII phosphorylation is complex, including enhanced SynGap activity (Walkup IV et al., 2015) and dispersing SynGap from the spine (Araki et al., 2015). We evaluated the contribution of these processes by eliminating then individually. Simulations reveal that persistent activation of ERK requires autophosphorylation of CaMKII and dispersion of pSynGap to the dendrite (Figure 3F). A lower ppERK total activity results when pSynGap remains anchored in the spine. Blocking the phosphorylation of SynGap was implemented using two approaches (Figure 3F). In one, CaMKII can bind to SynGap but does not phosphorylate it. This reduces the available SynGap, which doubles ppERK concentration compared to control. In

the second approach, CaMKII is unable to bind to SynGap. This increases the available SynGap, resulting in a reduction of ppERK below basal. These data suggest that the quantity of free SynGap in the spine regulates ERK activation which is controlled by CaMKII. To verify that the results were not an artifact of the binding affinity implemented in the model, simulations were repeated using 10x and 100x lower affinity values. Simulation results show a similar relation of ppERK to pSynGap (results not shown), reinforcing the hypothesis that CaMKII regulates ppERK total activity through its modulation of SynGap.

Overall ppERK response is a linear combination of response to calcium and cAMP

Simulations reveal that both pathways (calcium, cAMP) combine linearly to activate ERK. Figure 4A shows that the response to stimulating both pathways overlaps with the sum of the single pathway responses. This summation was observed with short and long duration stimuli and with high and low amplitude stimulations, regardless of whether calcium, was below or above the threshold. When calcium is below threshold (e.g. short-duration stimuli), cAMP contributes more to ppERK, whereas when calcium is above the threshold, it provides most of the ppERK (Figure 4B).

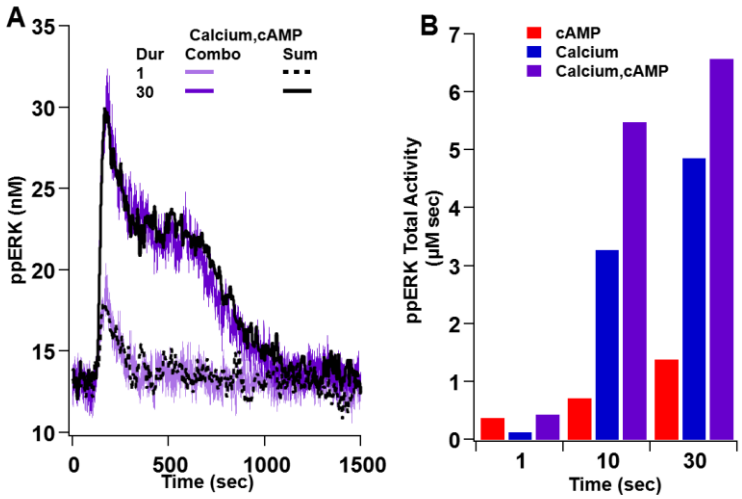

Figure 4: ***Overall ppERK response is linear combination of response to calcium and cAMP. A.*** *Time course of ppERK response to calcium and cAMP. Calcium in combination with cAMP traces overlaps with the sum of the single pathway responses for both short and long duration stimuli.* ***B.*** *Summary of ppERK AUC versus duration shows that the fraction of ppERK produced by calcium pathways increases with duration of the stimulation.*

In summary, ppERK exhibits a non-linear response to calcium, a linear response to cAMP pathways, and the response to the combination of pathways also is a linear combination of

the single pathway responses. However, these simulations used single pulses of stimuli; thus, the next section evaluates the response to stimuli similar to those used for synaptic plasticity experiments.

L-LTP stimuli: ERK signaling pathway temporally integrate input signal

Studies have demonstrated that ERK contributes to L-LTP through initiating local protein synthesis in dendrites and spines and controlling of transcription in the nucleus. Previous research has shown that different temporal patterns for inducing LTP work through different signaling pathways: PKA is needed for spaced stimuli while CaMKII is greater in response to massed stimuli. Thus, a critical question is whether different temporal patterns select different signaling pathways for activation of ERK. To evaluate that question, we simulated the response to L-LTP inputs. As in LTP experiments, the model was activated with four trains of 100 Hz stimuli for 1 sec using a range of inter-train intervals (ITIs), including massed (3,20,40 sec) and spaced (80,300 sec) ITI.

Temporal sensitivity of ppERK to cAMP matches that of PKA

Since ppERK increases more with cAMP duration than concentration (either direct action or in combination with Giβγ), as shown above, we predicted that ppERK would be greater for spaced than massed stimulation with cAMP. Model simulations with cAMP input show a preference for prolonged ITI as predicted. Figure 5A, B shows that ppERK total activity increases as ITI increases. Note that the ppERK amplitude decreases with ITI (Figure 5A), but the increase in ppERK duration more than compensates for the lower amplitude, resulting in greater total activity for the 300 sec ITI. This is due to sublinear summation observed for ITI up to 80 sec: ppERK in response to Giβγ plus direct cAMP is less than the sum of the responses to either pathway alone up to 80 sec (Figure 5B), similar to that observed with long-duration single-pulse stimuli. Competition for Src and Rap1GDP, which limits linear summation for long-duration stimuli, is also observed for L-LTP stimuli. This competition is not observed with very long ITI (300 sec) because most molecule quantities return to basal between stimuli, restoring the system to its initial state. Thus, the response to 4 trains separated by 300 sec is ~4 times the response to a single train. Note that the temporal sensitivity of ppERK is similar to that of PKA

as observed in Figure 5B. However, the Epac pathway contributes more to ppERK with short ITI while PKA contributes more with space stimuli, suggesting an Epac dependent L-LTP. In summary, ERK activated by cAMP exhibits sensitivity to ITI and is greater with spaced stimuli. These data are consistent with experiments showing a requirement for PKA in spaced but not massed stimulation, and simulations showing an increase in PKA activity with spaced stimulation (Kim et al., 2010; Woo et al., 2003).

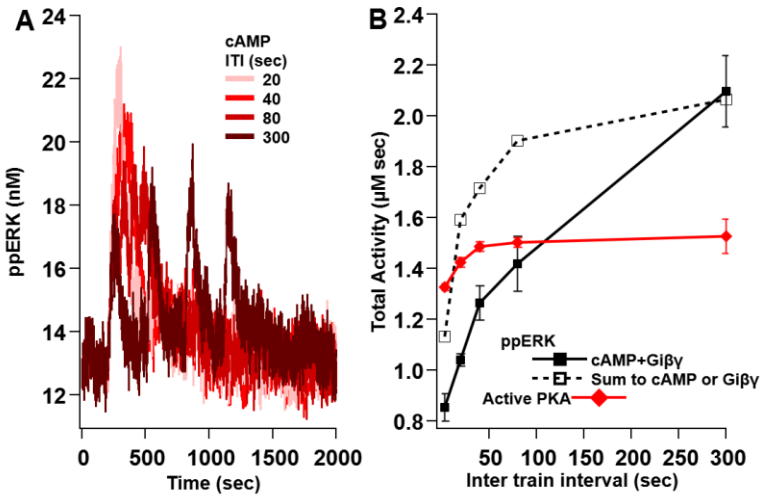

Figure 5: ***ppERK favors spaced stimuli in response to cAMP input: A.*** *Time course of ppERK in response to 4 trains of 100 Hz stimuli of cAMP (direct and indirect pathways). ppERK peak amplitude decreases with ITI, but the AUC increases with ITI.* ***B****. Total kinase activity in response to cAMP shows that ppERK exhibits sublinear response to direct and indirect cAMP stimuli: the sum (dashed line) is higher than ppERK in response to combination (solid black line) for all but the longest ITI. PKA and ppERK have similar temporal sensitivity, favoring spaced stimuli.*

ppERK favors longer ITIs, independent of CaMKII temporal sensitivity

L-LTP simulations using 1 μM amplitude calcium pulses produce similar ppERK traces for ITIs between 3 and 40 sec, with 80 sec ITI slightly prolonging the ppERK response (Figure 6A). Multiple 1 sec pulses of 1 μM calcium are similar to a single 4 sec pulse, due to the slow decay of pCaMKII; thus, calcium is above the threshold for CaMKII ultrasensitivity and ppERK is sustained for a long duration. Only with a 300 sec ITI does pCaMKII and ppERK decay (though not to basal) between stimuli. The temporal sensitivity of ppERK in response to calcium input tends toward longer ITIs than the temporal sensitivity of CaMKII. The greatest total activity of ppERK (Figure 6B) and pCaMKII (Figure 6C) are observed with 80 sec ITI. To test

the role of CaMKII ultrasensitivity in the temporal sensitivity of ppERK, we repeated simulations with an increased PP1 quantity (10 µM, or 50% ratio). As shown in Figure 6C, the increased PP1 changes the temporal sensitivity of CaMKII, with the greatest quantity occurring with short ITIs, as reported previously (Ajay and Bhalla, 2004; Kim et al., 2010). This change shifted ppERK temporal sensitivity slightly to favor middle ITIs, but still does not match the temporal sensitivity of CaMKII.

In addition to varying PP1 quantity, we used lower calcium pulses and an alternative CaMKII model (Dupont et al., 2003; Jędrzejewska-Szmek et al., 2017) that does not exhibit the same ultrasensitivity. Simulations with this alternative CaMKII model reveal a small shift in temporal sensitivity toward smaller ITIs, but the temporal sensitivity of ppERK still tends toward longer ITIs than the temporal sensitivity of CaMKII. Similar results were observed with the ultrasensitive CaMKII model when smaller calcium pulses (0.5 µM) were used (Figure 6B&C). In addition, ERK's temporal sensitivity follows RasGRF (low calcium) and SynGap (high calcium) temporal activity (results not shown). In summary, though the ultrasensitivity of CaMKII is controlled in part by PP1, ppERK temporal sensitivity does not follow CaMKII temporal sensitivity, and instead follows the temporal sensitivity of CaMKII downstream targets.

ppERK favors long intertrial intervals

L-LTP simulations with both calcium and cAMP show an increase of ppERK total activity with longer ITI. Figure7A shows that, using 18% PP1 and 1 µM calcium (above threshold), the greatest total ppERK occurs at 80 sec, while greatest total ppERK is observed at 300 sec with 50% PP1-1 µM calcium and 18% PP1-0.5 µM calcium (below threshold). Though the change in optimal ITI varies little, the total quantity of ppERK greatly depends on calcium and PP1 concentration. In these simulations, the contribution of the cAMP pathway to ppERK is independent of calcium; cAMP is responsible for a majority of the ppERK with below threshold calcium, but only responsible for a third of the ppERK for above threshold calcium (Figure7B).

ppERK linearly integrates the calcium and cAMP inputs when calcium is below threshold. Thus, the response to the combined stimuli is similar to the sum of ppERK responses to individual stimuli with 0.5 µM calcium (Figure7A). An ANOVA, with ITI and type (combination versus summation) as factors, shows that ITI is significant ($P < 0.0001$) but not type (P 0.0658).

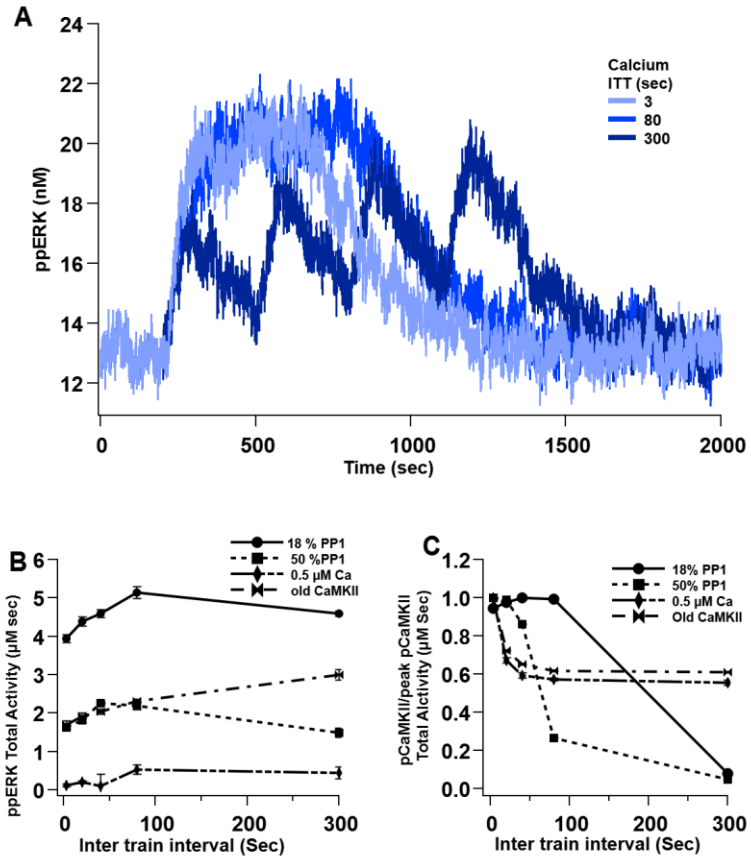

Figure 6: ***ppERK favors spaced stimuli in response to calcium input, in contrast to temporal sensitivity of CaMKII. A.*** *Time course of ppERK in response to 4 trains of 100 Hz calcium stimuli (1 µM conc) shows sustained and prolong ppERK with 3 and 80 sec ITI.* ***B.*** *ppERK AUC changes with PP1 quantity, but still is highest for 80 or 300 s ITIs.* ***C.*** *Increasing PP1 quantity or lowering calcium concentration makes CaMKII more sensitivity to shorter ITIs.*

Similar results were obtained with 50% PP1 and above threshold calcium, with the possible exception of the 20 sec ITI. Different results were observed with above threshold calcium, as both ITI and type were significant (P <0.0001). In fact, a supralinear summation was observed: the response of the combination is greater than the summation of individual responses up to 80 sec ITI (Figure 7A). CaMKII modulation of SynGap with above threshold calcium may be responsible as it enhances RasGTP and Rap1GTP in response to cAMP.

In summary, these results demonstrate that ERK signaling pathways integrates and consolidates multiple inputs synergistically. In fact, ppERK activity in response to the combination of calcium and cAMP is always greater than the response to either calcium or cAMP alone. For high calcium inputs, as likely occur during L-LTP induction, these inputs combine supralinearly for all but the longest ITIs. To address the question of which pathway

contributes more to ppERK and whether different temporal patterns use different pathways, we calculated the percent ppERK produced by cAMP versus calcium. Note that this analysis is qualitative due to the supralinear summation. The contribution of the calcium pathway relative to the cAMP pathway is greatest when calcium is above threshold for an ultrasensitive CaMKII response (Figure 7B). Nevertheless, as ITIs increase, calcium contribution decreases, and cAMP contribution increases regardless of PP1 concentration (Figure 7C&D). In conclusion, the contribution of cAMP is greater with longer ITI while calcium contribution is decreasing with prolonged ITIs.

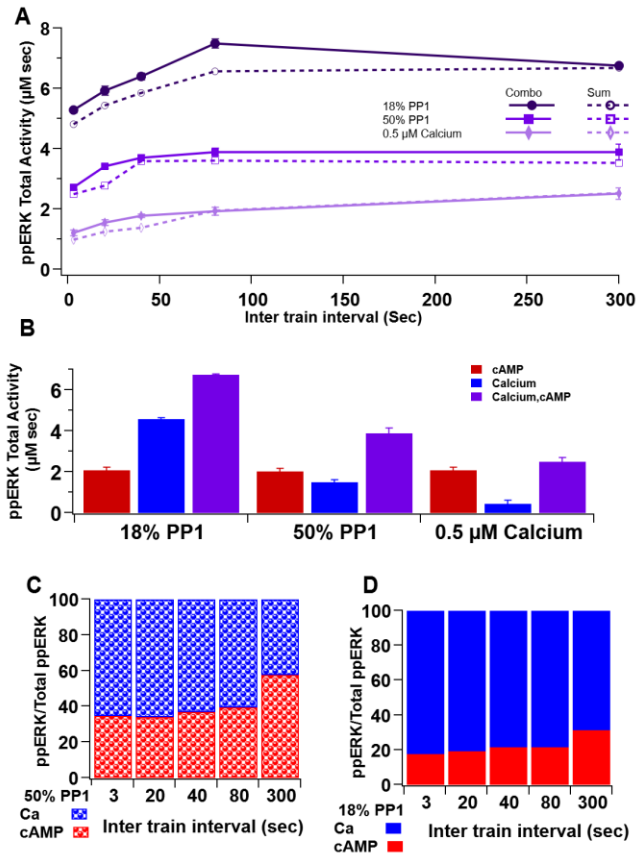

Figure 7: ***ppERK integration of calcium and cAMP inputs can be linear or supralinear.*** *(**A**) ppERK mostly increases with temporal interval with the greatest quantity occurring at 80 sec (above threshold or 18% PP1) or 300 sec (below threshold or low calcium). Linear summation occurs at low calcium or high PP1 – conditions that reduce ultrasensitivity of CaMKII (Figure 3E). Supralinear summation occurs at 18% PP1, and at 20 sec ITI for 50% PP1.* ***B.*** *Summary plot of ppERK total activity in response to 300 sec ITI. The contribution of the calcium pathway relative to the cAMP pathway is greatest when calcium is above threshold for an ultrasensitive CaMKII response.* ***C&D****. Qualitative normalized single contribution over multiple pathways. Calcium contribution decreases, and cAMP contribution increases with increase ITIs, for both 50%* ***(C)*** *and 18%* ***(D)*** *PP1 concentration.*

Robustness

In computational models it is critical to ensure the robustness of the results to variation in parameter values. The main result of the model is that ERK signaling pathways, no matter the protocol used, favor spaced stimuli. To assess the robustness of the temporal sensitivity of ERK signaling pathway to small variations in parameters, simulations were repeated using concentrations of ±10% of the control value. The concentrations were changed either individually or collectively with changes drawn from a uniform distribution (between -10% and +10%). These robustness simulations show that total ERK increase with ITI, similar to control results. Table 4 shows that preferred the ITI is 80 sec 67 % of the time, followed by 300 sec 30% of the time. Thus, the model prediction of ERK temporal sensitivity is robust to small variations in parameters.

We also evaluated the change in the maximum AUC (over all 5 ITIs) minus the minimum AUC (i.e. AUC range), compared to the control. Figure 8 shows that increasing the concentration of the molecules has little to no effect, while a decrease of a few molecules greatly increased the range. The largest changes were caused by decreases in calcium buffers, which allows calcium concentration to increase, and decreases in GAPs, such as SynGap, which allows an increase in RasGTP and Rap1GTP. A reduction in any of these molecules increased the AUC range by increasing the maximum AUC. This is consistent with results showing that an increase in calcium increased ppERK. On the other side, cAMP and cAMP pathway molecules seem to have no effect on the AUC range, and mostly just change the basal ppERK. The effect of random changes to the entire set of molecules was analyzed by random forest regression. Table 5 shows the molecules the cause the most significant change to the AUC range. Many of the molecules whose variation causes a large effect when changed individually are significant. For example, calbindin and other molecules that control calcium concentration (NCX, leak) are ranked high by the random forest regression. On the other hand, the phosphatase for ERK (MKP1), phosphodiesterases that control cAMP (PDE4 and PDE2) are ranked high by the random forest regression but have small effects when varied alone. Opposite results are observed with SynGap, losing it importance when other molecules are simultaneously varied, possibly because increases in other GAPs can compensate. In summary, despite the changes in AUC caused by changes in parameters, the temporal sensitivity of ERK is quite robust and still favors spaced ITIs.

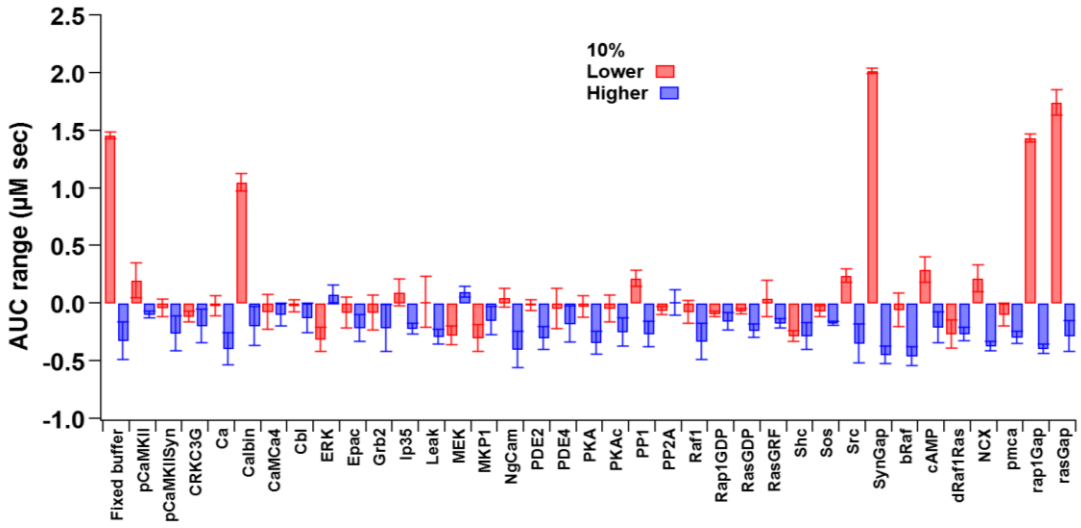

Figure 8: ***Calcium buffers and Gaps affect the measure of variance****: Molecules concentration were changed individually by either +10% (blue) or -10% (red). AUC range (max - min) of each set was normalized by the control. The most impacting molecules are calcium buffer such as fixed buffer, calbindin, and GAPs such as SynGap, Rap1Gap and RasGap. Decreasing the molecules concentration has a greater effect on the AUC variance than increasing the concentration. See Table 5 for list of abbreviations.*

Table 4: ***Count of Best ITIs****: count of preferred ITIs in robustness simulations, using either single molecule changes of +/- 10% or random changes (between +10% and -10%) to all molecules.*

ITIs	Random	10 % lower	10% higher	Total percent
40	8	7	5	3.83
80	199	62	87	66.67
300	93	42	19	29.50

Discussion

Numerous experiments have demonstrated that ERK is critical in L-LTP induction; however, the relative importance of the wide variety of signaling molecules and pathways that activate ERK is unclear. Using a computational model of signaling pathways underlying L-LTP in hippocampus CA1, we evaluated whether different L-LTP stimulation frequencies utilized different pathways and whether synergy between pathways occurs. Our results demonstrate that ERK activation with single pulse stimuli exhibits a non-linear response to calcium via CaMKII, but a linear response to cAMP via Epac and PKA. We also investigated the activation of ERK in

Table 5: ***Random forest analysis:*** *Molecules were randomly simultaneous changed by either +10% or -10%. Features are ranged from most important to least important in predicting the temporal sensitivity.*

Molecules abbreviation	**Weights**	**Molecules full name**
pCaMKII	4.200	Phosphorylated Calcium Calmodulin-dependent Kinase II
Calbin	3.251	Calbindin
Rap1GDP	2.785	Ras-Proximate-1 GDP
MKP1	2.486	Mitogen-activated protein Kinase Phosphatase 1
dRaf1Ras	2.424	Dimerized RafRasGTP
Leak	1.685	Calcium Leak
Cbl	1.578	E3 ubiquitin-protein ligase CBL or Casitas B-lineage Lymphoma
PDE4	1.521	Phosphodiesterase 4
Epac	1.345	Exchange Protein directly Activated by cAMP
NCX	1.309	Sodium Calcium Exchanger
rasGap	1.265	Ras GTPase Activating Protein
PDE2	1.083	Phosphodiesterase 2
Src	0.920	Non-Receptor Tyrosine Kinase
PP2A	0.850	Protein Phosphatase 2
CRK/C3G	0.769	v-CRK Proto-Oncogene/Rap guanine nucleotide exchange factor 1
PKAc	0.726	Protein Kinase A catalytic subunit
CamCa4	0.674	Calmodulin bind to calcium
SynGap	0.666	Synaptic rasGap
PKA	0.513	Protein Kinase A
pmca	0.487	Plasma membrane calcium pump
PP1	0.480	Protein phosphatase 1
Shc	0.469	Src homology collagen-like
bRaf	0.462	Raf proto-oncogene, serine/threonine kinase
NgCam	0.364	Calmodulin bound Neurogranin
MEK	0.348	Mitogen-activated protein Kinase Kinase
RasGDP	0.340	Ras protein GDP
Ca	0.289	Calcium
Fixed buffer	0.260	Immobile calcium buffer
cAMP	0.234	Cyclic adenosine monophosphate
pCaMKIISyn	0.228	Phosphorylated Calcium Calmodulin-dependent Kinase II bound to Synaptic rasGap
Sos	0.097	Son of Sevenless
RasGRF	0.046	Ras guanine nucleotide–releasing factor
ERK	0.046	Mitogen-activated protein Kinase

response to L-LTP stimulation consisting of four trains of 100 Hz stimuli separated by different intertrial intervals. We found that ppERK in these stimuli is maximal at 80-300 sec ITIs, confirming that ERK slowly integrates its inputs. The response to the combination of cAMP and calcium inputs is linear for low calcium but supralinear for high calcium due to CaMKII mediated reduction in SynGap activity. In addition, calcium contributes more to ERK for massed stimuli whereas cAMP contributes more to ERK for spaced stimuli.

The model elucidates that CaMKII contributes to ERK activation through phosphorylation of SynGap. This synaptic RasGap, selectively expressed in the brain, regulates ERK activity by exhibiting GTPase activity towards RasGTP and Rap1GTP (Pena et al., 2008). CaMKII phosphorylation of SynGap both increases its Gap activity (Walkup IV et al., 2015) and causes dispersion to the dendrite (Araki et al., 2015). To investigate the role of dispersion, we repeated simulations without dispersion of pSynGap and observed that the ppERK amplitude was decreased by half. This effect is observed because the Gap activity is doubled in the spine, reducing the available quantity of RasGTP and Rap1GTP. Thus, the dispersion of pSynGap attenuates the Gap activity in the spine, which allows a long-lasting spine enlargement as observed in experiments (Araki et al., 2015). We evaluated the effect of enhanced SynGap activity using two different methods. Blocking CaMKII binding to SynGap greatly reduced ppERK activity, because of increased free SynGap in the spine. This result is consistent experiments (Rumbaugh et al., 2006) showing that overexpression of SynGap significantly reduced ERK activity. In contrast, allowing CaMKII to bind SynGap but not phosphorylate it greatly increased ppERK activity, due to decreased free SynGap – in essence, CaMKII traps SynGap which enhances ppERK activity. This result also is consistent experiments (Rumbaugh et al., 2006) showing that SynGap depletion enhanced ppERK activity. Thus, CaMKII influences ERK activation indirectly through SynGap phosphorylation.

The temporal sensitivity of ERK in response to L-LTP stimulation is similar to that of PKA and different from that of CaMKII. Our results show that ERK activity in response to L-LTP induction increases with ITIs. This result is consistent with experimental data (Ajay and Bhalla, 2004), showing that the greatest ppERK activity is seen with spaced stimuli. This temporal sensitivity of ppERK matches that of PKA, as we observed maximal activity of both with spaced stimuli. The increase in PKA activity in response to spaced stimuli is similar to that

observed previously (Kim et al., 2010). The observation that the cAMP pathway contribution to ERK increases with long ITIs is consistent with experimental studies which found PKA dependence with spaced stimuli (Woo et al., 2003). The temporal sensitivity of ppERK does not match that of CaMKII total activity, which is greater with shorter ITIs. This observation is similar to experimental and computational studies (Ajay and Bhalla, 2004; Kim et al., 2010) showing a decrease in CaMKII with spaced stimuli. A consequence is that the contribution of calcium pathways to ppERK decreases with longer ITIs.

Several models have evaluated the molecular dependence and temporal sensitivity of ERK in L-LTP induction. The most comprehensive model of ERK signaling pathways in neurons (Ajay and Bhalla, 2004) shows that ppERK temporal sensitivity is opposite to that of PKA and CaMKII. Our results agree with Ajay and Bhalla (2004) regarding the temporal sensitivity of ppERK and CaMKII, but seemingly differ for PKA. This is due to the method for measuring temporal sensitivity, because using activity peak instead of total activity (AUC) reveals a decrease in PKA activity with increased ITIs in our results, similar to Ajay and Bhalla (2004). This reveals that, in some cases, temporal sensitivity depends on the measure of activity. Other models have investigated the importance of feedforward loops in activating ERK during LTP induction in CA1. Ajay and Bhalla (2004) show L-LTP stability is maintained by the feedforward loops involving PKMζ, the atypical form of PKC. Alternatively, Neves et al. (2008) show that spatial patterns of ppERK activity require feedforward loops involving PKA. In agreement with their results, our model has a feedforward loop connecting CaMKII to SynGap to ERK, which is sufficiently activated with L-LTP induction. This pathway may be critical for induction of L-LTP in CA1 for protocols resistant to inhibition of PKC (Sweatt, 1999). In summary, our study supports prior results showing that feedforward loops are sufficient to activate ERK but reveals a novel feedforward loop involving SynGap.

Understanding signaling pathways that activate ERK during induction of L-LTP is crucial for understanding mechanisms underlying learning and memory. MEK inhibitors, which block phosphorylation of ERK, impair learning and memory in diverse behaviors (Saeed et al., 2018; Selcher et al., 2003, 1999). Similarly, MEK inhibition blocks L-LTP in hippocampal CA1 in response to 1 train of 100 Hz stimulation plus Epac activation (Gelinas et al., 2008), 5 Hz stimulation plus βAR agonists (Winder et al., 1999), theta-burst stimulation (Shalin et al., 2006)

and spaced 100 Hz stimulation (English and Sweatt, 1997; Kelleher et al., 2004). This latter also demonstrates that inhibition of ERK 30 minutes after induction does not block LTP, consistent with our observation that ppERK returns to basal after 30 min. ERK contributes to L-LTP and memory through several mechanisms, including protein synthesis (Connor et al., 2012; Kelleher et al., 2004), regulation of AMPA receptor recruitment to synapses following LTP induction (Qin et al., 2005; Zhu et al., 2002) and enhanced action potential firing during theta-burst stimulation (Selcher et al., 2003). These different mechanisms may require different pools of ERK, a subject for future investigation. Our results showing that spaced stimulation produces greater ERK activity have interesting connections with memory storage. More effective learning has been observed in spaced training (Genoux et al., 2002). Thus, our data suggest that repetitive and space training may improve learning due to enhanced ERK activity.

ppERK can translocate to the nucleus and initiate gene transcription or stay in the cytoplasm and initiate local changes in excitability. Studies have shown that scaffolding proteins, such as Kinase Suppressor of Ras (KSR) protein (Dougherty et al., 2009; Shalin et al., 2006) and β-arrestins (Bourquard et al., 2015; DeFea et al., 2000), can create multi-protein complexes of ERK, MEK and Raf, and dictate the subcellular location of ERK activity. Thus, a critical question is whether the spatial pool of ERK depends on which signaling pathways are activated during induction of LTP. These different pools of ERK may perform different functions, as mentioned above and in the context of the tagging and capture hypothesis for L-LTP induction. The tagging and capture hypothesis explains that stimulated spines are marked (tagged), which enables them, but not non-stimulated spines, to capture newly synthesized proteins (Frey and Morris, 1997; Sajikumar et al., 2007; Young et al., 2006) to enable persistence of L-LTP. Phospho-proteins, including a pool of ppERK in the spine, may be part of that tag (Redondo et al., 2010). This leads to a second question regarding what limits the spatial spread of molecules involved in tagging. In this context, a possible role for SynGAP dispersion would be to limit diffusion of active Ras family proteins to nearby, non-stimulated spines, thereby creating microdomains. Spatial models (Ajay and Bhalla, 2007; Neves et al., 2008) have shown different mechanisms that form microdomains, though none as small as single spines. Other spatial models (Kim et al., 2010) of PKA and CaMKII signaling pathways reveal spine-sized microdomains of cAMP, but not PKA, suggesting additional mechanisms may be needed to produce spine-sized microdomains of ERK. Taking those questions together it will be quite

interesting to implement a spatial model to investigate mechanisms that govern spatial pools of ERK and spatial and tagging specificity.

METHODS

Computational methods

To investigate how temporal pattern of synaptic activity determines which pathway in the ERK signaling cascade (Figure

1A) dominates in dendritic spines of hippocampal CA1 pyramidal neurons, we developed a single compartment, stochastic reaction-diffusion model of pathways activating ERK. The model was built by merging and adapting two existing models of synaptic plasticity in hippocampal neurons. One of those models (Jędrzejewska-Szmek et al., 2017) explains how different temporal patterns activate different kinases such as CaMKII and PKA that are critical for L-LTP induction, and the other model (Jain and Bhalla, 2014) demonstrates that protein synthesis is the result of synergistic activation of different pathways such as ERK and mTOR to generate unique patterns in response to different L-LTP stimuli. These previously published models were modified by adding several molecules and reactions critical for ERK activation.

One major change to the merged model is C-Raf dimerization. Dimerization regulates C-Raf activation and its subcellular localization (Desideri et al., 2015; Garnett et al., 2005). Full activation of C-Raf, but not B-Raf, requires dimerization. RasGTP binds to C-Raf to form an inactive complex, C-Raf-RasGTP, which then homodimerizes to become active, thus able to phosphorylate MEK that activates ERK. Another major change is the addition of two important molecules, RasGRF and SynGap, involved in hippocampal LTP (Araki et al., 2015; Darcy et al., 2014; Jin and Feig, 2010; Kim et al., 2003, 1998; Li et al., 2006). RasGRF is activated by binding to calcium-calmodulin; once activated, RasGRF binds to RasGDP and allows the exchange of GDP for GTP. SynGap inactivates Rap1GTP and RasGTP with low affinity. Once phosphorylated by CaMKII, SynGAP affinity doubles towards RasGTP and Rap1GTP and causes SynGAP dispersion from synapses to the dendrite.

Initial conditions and rate constants are either taken from previous models (Jain and Bhalla, 2014; Jędrzejewska-Szmek et al., 2017) or adjusted to reproduce experimentally measured concentrations of molecules. The concentration of some species was adjusted to

produce an intracellular concentration of calcium of ~50 nM and cAMP of ~30 nM, among others. For example, the concentration of PDEs was adjusted to produce a 30 nM basal of cAMP. Calcium extrusion mechanisms and the low affinity and immobile calcium buffer were adjusted to obtain a steady-state of about 50 nM of internal calcium. To match the *in vitro* data on basal concentration, we ran the model for about an hour to obtain steady-state concentrations for all molecules.

Several simulations use a compartment with a volume comparable to a spine head (about 0.1 to 0.8 μm^3). To minimize noise inherent in stochastic models, most simulations used a larger compartment, of volume 4 μm^3. Other than the level of noise, no differences in temporal sensitivity were observed between the small and large volume models.

Stimulation protocols

In brain slices, presynaptic stimulation results in calcium influx through NMDA receptors, and release of norepinephrine (NE) or dopamine, which bind to Gs-coupled metabotropic receptors (Jędrzejewska-Szmek et al., 2017). To investigate the effect of calcium distinct from cAMP produced by NE, the model is activated using three independent inputs leading to ERK activation: calcium (through RasGRF and SynGap), cAMP (through Epac and PKA), and βγ subunit of Gi (through implicit PKA phosphorylation of βAR). To determine if maximal ERK activation requires multiple pathways, the contribution of each pathway was tested singly and in combination using either a duration or amplitude protocol (Table 1). Duration protocols used a sustained concentration of calcium, cAMP, and Giβγ. Amplitude protocols used transient (1 sec duration) elevations of different concentrations of the inputs. Calcium and cAMP each have several different pathways to ERK activation; thus, to determine the contribution of each of the (sub)pathways, the above simulations were repeated with one of the rates set to zero, as shown in Table 2.

To investigate whether different L-LTP temporal patterns select different signaling pathways for ERK activation, simulations were performed using stimulation protocols identical to the experimental protocols used to induce L-LTP. Therefore, we stimulated the model with four trains of 100 Hz for 1 sec at five different intertrial intervals: 3, 20, 40sec (massed) or 80 and 300 sec (spaced) (Figure 1C). Each stimulation pulse triggered a transient release of either calcium, cAMP (direct action, and in combination with Giβγ) singly or in combination.

Simulation and Analysis

The model is implemented using a stochastic reaction-diffusion simulator NeuroRD (Jędrzejewski-Szmek and Blackwell, 2016), version 3.2.4 (https://github.com/neurord/stochdiff/releases), using the adaptive (asynchronous tau-leap) numerical method and tolerance of 0.1. All model files needed to run the simulations or examine molecules quantities or reactions rate constants are available on GitHub (https://github.com/neurord/ERK).

Biochemical experiments assess kinase activity by measuring the change in concentration of the product after a specific time. Thus, in these simulations, the kinase activity is quantified as total activity over simulated time compared to the activity under conditions of no stimulation, also known as Area Under the Curve (AUC). To account for stochastic variation, simulations were repeated five times and results presented are the mean and standard error over the trials. Analysis was done in Python 3, using nrdh5_anal.py available on github (https://github.com/neurord/NeuroRDanal). The test of linearity in Figure 6A was by analysis of variance using SAS version 9.4, using AUC of doubly phosphorylated ERK (ppERK) as the dependent variable, and intertrial interval and stimulation type (combination or summation) as independent variables. Random forest regression (implemented in Python3, https://github.com/neurord/ERK/tree/master/Analysis) was used for sensitivity analysis, to determine which parameter values had the most influence on the change in ppERK AUC versus ITI.

REFERENCES

Ajay, S.M., Bhalla, U.S., 2007. A propagating ERKII switch forms zones of elevated dendritic activation correlated with plasticity. HFSP J 1, 49–66. https://doi.org/10.2976/1.2721383

Ajay, S.M., Bhalla, U.S., 2004. A role for ERKII in synaptic pattern selectivity on the time-scale of minutes. European Journal of Neuroscience 20, 2671–2680. https://doi.org/10.1111/j.1460-9568.2004.03725.x

Araki, Y., Hong, I., Gamache, T.R., Ju, S., Collado-Torres, L., Shin, J.H., Huganir, R.L., 2020. SynGAP isoforms differentially regulate synaptic plasticity and dendritic development. Elife 9. https://doi.org/10.7554/eLife.56273

Araki, Y., Zeng, M., Zhang, M., Huganir, R.L., 2015. Rapid Dispersion of SynGAP from Synaptic Spines Triggers AMPA Receptor Insertion and Spine Enlargement during LTP. Neuron 85, 173–189. https://doi.org/10.1016/j.neuron.2014.12.023

Bourquard, T., Landomiel, F., Reiter, E., Crépieux, P., Ritchie, D.W., Azé, J., Poupon, A., 2015. Unraveling the molecular architecture of a G protein-coupled receptor/β-arrestin/Erk module complex. Scientific Reports 5, 10760. https://doi.org/10.1038/srep10760

Bradshaw, J.M., Kubota, Y., Meyer, T., Schulman, H., 2003. An ultrasensitive Ca2+/calmodulin-dependent protein kinase II-protein phosphatase 1 switch facilitates specificity in postsynaptic calcium signaling. Proc Natl Acad Sci USA 100, 10512–10517. https://doi.org/10.1073/pnas.1932759100

Buscà, R., Pouysségur, J., Lenormand, P., 2016. ERK1 and ERK2 Map Kinases: Specific Roles or Functional Redundancy? Frontiers in Cell and Developmental Biology 4. https://doi.org/10.3389/fcell.2016.00053

Connor, S.A., Maity, S., Roy, B., Ali, D.W., Nguyen, P.V., 2012. Conversion of short-term potentiation to long-term potentiation in mouse CA1 by coactivation of β-adrenergic and muscarinic receptors. Learn. Mem. 19, 535–542. https://doi.org/10.1101/lm.026898.112

Darcy, M.J., Trouche, S., Jin, S.-X., Feig, L.A., 2014. Ras-GRF2 Mediates LTP, Survival and Response to an Enriched Environment of Newborn Neurons in the Hippocampus. Hippocampus 24, 1317–1329. https://doi.org/10.1002/hipo.22313

Davis, S., Vanhoutte, P., Pagès, C., Caboche, J., Laroche, S., 2000. The MAPK/ERK Cascade Targets Both Elk-1 and cAMP Response Element-Binding Protein to Control Long-Term Potentiation-Dependent Gene Expression in the Dentate Gyrus *In Vivo*. J. Neurosci. 20, 4563–4572. https://doi.org/10.1523/JNEUROSCI.20-12-04563.2000

de Rooij, J., Rehmann, H., van Triest, M., Cool, R.H., Wittinghofer, A., Bos, J.L., 2000. Mechanism of Regulation of the Epac Family of cAMP-dependent RapGEFs. J. Biol. Chem. 275, 20829–20836. https://doi.org/10.1074/jbc.M001113200

DeFea, K.A., Zalevsky, J., Thoma, M.S., Déry, O., Mullins, R.D., Bunnett, N.W., 2000. β-Arrestin–Dependent Endocytosis of Proteinase-Activated Receptor 2 Is Required for Intracellular Targeting of Activated Erk1/2. J Cell Biol 148, 1267–1282.

Desideri, E., Cavallo, A.L., Baccarini, M., 2015. Alike but Different: RAF Paralogs and Their Signaling Outputs. Cell 161, 967–970. https://doi.org/10.1016/j.cell.2015.04.045

Dougherty, M.K., Ritt, D.A., Zhou, M., Specht, S.I., Monson, D.M., Veenstra, T.D., Morrison, D.K., 2009. KSR2 is a calcineurin substrate that promotes ERK cascade activation in response to calcium signals. Mol. Cell 34, 652–662. https://doi.org/10.1016/j.molcel.2009.06.001

Dupont, G., Houart, G., De Koninck, P., 2003. Sensitivity of CaM kinase II to the frequency of Ca2+ oscillations: a simple model. Cell Calcium 34, 485–497. https://doi.org/10.1016/S0143-4160(03)00152-0

English, J.D., Sweatt, J.D., 1997. A Requirement for the Mitogen-activated Protein Kinase Cascade in Hippocampal Long Term Potentiation. J. Biol. Chem. 272, 19103–19106. https://doi.org/10.1074/jbc.272.31.19103

Enserink, J.M., Christensen, A.E., de Rooij, J., van Triest, M., Schwede, F., Genieser, H.G., Døskeland, S.O., Blank, J.L., Bos, J.L., 2002. A novel Epac-specific cAMP analogue demonstrates independent regulation of Rap1 and ERK. Nature Cell Biology 4, 901–906. https://doi.org/10.1038/ncb874

Frey, U., Morris, R.G.M., 1997. Synaptic tagging and long-term potentiation. Nature 385, 533–536. https://doi.org/10.1038/385533a0

Garnett, M.J., Rana, S., Paterson, H., Barford, D., Marais, R., 2005. Wild-Type and Mutant B-RAF Activate C-RAF through Distinct Mechanisms Involving Heterodimerization. Molecular Cell 20, 963–969. https://doi.org/10.1016/j.molcel.2005.10.022

Gelinas, J.N., Banko, J.L., Peters, M.M., Klann, E., Weeber, E.J., Nguyen, P.V., 2008. Activation of exchange protein activated by cyclic-AMP enhances long-lasting synaptic potentiation in the hippocampus. Learning & Memory 15, 403–411. https://doi.org/10.1101/lm.830008

Genoux, D., Haditsch, U., Knobloch, M., Michalon, A., Storm, D., Mansuy, I.M., 2002. Protein phosphatase 1 is a molecular constraint on learning and memory. Nature 418, 970–975. https://doi.org/10.1038/nature00928

Jain, P., Bhalla, U.S., 2014. Transcription Control Pathways Decode Patterned Synaptic Inputs into Diverse mRNA Expression Profiles. PLoS ONE 9, e95154. https://doi.org/10.1371/journal.pone.0095154

Jędrzejewska-Szmek, J., Luczak, V., Abel, T., Blackwell, K.T., 2017. β-adrenergic signaling broadly contributes to LTP induction. PLOS Computational Biology 13, e1005657. https://doi.org/10.1371/journal.pcbi.1005657

Jędrzejewski-Szmek, Z., Blackwell, K.T., 2016. Asynchronous τ-leaping. The Journal of Chemical Physics 144, 125104. https://doi.org/10.1063/1.4944575

Jin, S., Feig, L.A., 2010. Long-Term Potentiation in the CA1 Hippocampus Induced by NR2A Subunit-Containing NMDA Glutamate Receptors Is Mediated by Ras-GRF2/Erk Map Kinase Signaling. PLoS One 5. https://doi.org/10.1371/journal.pone.0011732

Kelleher, R.J., Govindarajan, A., Jung, H.-Y., Kang, H., Tonegawa, S., 2004. Translational control by MAPK signaling in long-term synaptic plasticity and memory. Cell 116, 467–479. https://doi.org/10.1016/s0092-8674(04)00115-1

Khalilimeybodi, A., Daneshmehr, A., Sharif-Kashani, B., 2018. Investigating β-adrenergic-induced cardiac hypertrophy through computational approach: classical and non-classical pathways. J Physiol Sci 68, 503–520. https://doi.org/10.1007/s12576-017-0557-5

Kim, J.H., Lee, H.-K., Takamiya, K., Huganir, R.L., 2003. The Role of Synaptic GTPase-Activating Protein in Neuronal Development and Synaptic Plasticity. J. Neurosci. 23, 1119–1124. https://doi.org/10.1523/JNEUROSCI.23-04-01119.2003

Kim, J.H., Liao, D., Lau, L.-F., Huganir, R.L., 1998. SynGAP: a Synaptic RasGAP that Associates with the PSD-95/SAP90 Protein Family. Neuron 20, 683–691. https://doi.org/10.1016/S0896-6273(00)81008-9

Kim, M., Huang, T., Abel, T., Blackwell, K.T., 2010. Temporal Sensitivity of Protein Kinase A Activation in Late-Phase Long Term Potentiation. PLoS Computational Biology 6, e1000691. https://doi.org/10.1371/journal.pcbi.1000691

Koch, W.J., Hawes, B.E., ALLENt, L.F., Lefkowitz, R.J., 1994. Direct evidence that Gi-coupled receptor stimulation of mitogen-activated protein kinase is mediated by GBy activation of p2lras. Cell Biology 91, 12706–12710.

Komiyama, N.H., Watabe, A.M., Carlisle, H.J., Porter, K., Charlesworth, P., Monti, J., Strathdee, D.J.C., O'Carroll, C.M., Martin, S.J., Morris, R.G.M., O'Dell, T.J., Grant, S.G.N., 2002. SynGAP Regulates ERK/MAPK Signaling, Synaptic Plasticity, and Learning in the Complex with Postsynaptic Density 95 and NMDA Receptor. J Neurosci 22, 9721–9732. https://doi.org/10.1523/JNEUROSCI.22-22-09721.2002

Li, S., Tian, X., Hartley, D.M., Feig, L.A., 2006. Distinct Roles for Ras-Guanine Nucleotide-Releasing Factor 1 (Ras-GRF1) and Ras-GRF2 in the Induction of Long-Term Potentiation and Long-Term Depression. J Neurosci 26, 1721–1729. https://doi.org/10.1523/JNEUROSCI.3990-05.2006

Lin, C.-H., Yu, M.-C., Chiang, C.-C., Bien, M.-Y., Chien, M.-H., Chen, B.-C., 2013. Thrombin-induced NF-κB activation and IL-8/CXCL8 release is mediated by c-Src-dependent Shc, Raf-1, and ERK pathways in lung epithelial cells. Cellular Signalling 25, 1166–1175. https://doi.org/10.1016/j.cellsig.2013.01.018

Luttrell, L.M., Della Rocca, G.J., van Biesen, T., Luttrell, D.K., Lefkowitz, R.J., 1997. Gβγ subunits mediate Src-dependent phosphorylation of the epidermal growth factor receptor. A scaffold for G protein-coupled receptor-mediated Ras activation. J. Biol. Chem. 272, 4637–4644. https://doi.org/10.1074/jbc.272.7.4637

Miningou, N., Blackwell, K.T., 2020. The road to ERK activation: Do neurons take alternate routes? Cellular Signalling 68, 109541. https://doi.org/10.1016/j.cellsig.2020.109541

Neves, S.R., Tsokas, P., Sarkar, A., Grace, E.A., Rangamani, P., Taubenfeld, S.M., Alberini, C.M., Schaff, J.C., Blitzer, R.D., Moraru, I.I., Iyengar, R., 2008. Cell Shape and Negative Links in Regulatory Motifs Together Control Spatial Information Flow in Signaling Networks. Cell 133, 666–680. https://doi.org/10.1016/j.cell.2008.04.025

Pena, V., Hothorn, M., Eberth, A., Kaschau, N., Parret, A., Gremer, L., Bonneau, F., Ahmadian, M.R., Scheffzek, K., 2008. The C2 domain of SynGAP is essential for stimulation of the Rap GTPase reaction. EMBO Rep 9, 350–355. https://doi.org/10.1038/embor.2008.20

Peng, S., Zhang, Y., Zhang, J., Wang, H., Ren, B., 2010. ERK in Learning and Memory: A Review of Recent Research. Int J Mol Sci 11, 222–232. https://doi.org/10.3390/ijms11010222

Qin, Y., Zhu, Y., Baumgart, J.P., Stornetta, R.L., Seidenman, K., Mack, V., van Aelst, L., Zhu, J.J., 2005. State-dependent Ras signaling and AMPA receptor trafficking. Genes Dev 19, 2000–2015. https://doi.org/10.1101/gad.342205

Rangamani, P., Levy, M.G., Khan, S., Oster, G., 2016. Paradoxical signaling regulates structural plasticity in dendritic spines. PNAS 113, E5298–E5307. https://doi.org/10.1073/pnas.1610391113

Redondo, R.L., Okuno, H., Spooner, P.A., Frenguelli, B.G., Bito, H., Morris, R.G.M., 2010. Synaptic tagging and capture: differential role of distinct calcium/calmodulin kinases in protein synthesis-dependent long-term potentiation. J. Neurosci. 30, 4981–4989. https://doi.org/10.1523/JNEUROSCI.3140-09.2010

Rumbaugh, G., Adams, J.P., Kim, J.H., Huganir, R.L., 2006. SynGAP regulates synaptic strength and mitogen-activated protein kinases in cultured neurons. Proceedings of the National Academy of Sciences 103, 4344–4351. https://doi.org/10.1073/pnas.0600084103

Saeed, M., Ghadiri, A., Hadizadeh, F., Attaranzadeh, A., Alavi, M.S., Etemad, L., 2018. Cinnamaldehyde improves methamphetamine-induced spatial learning and memory deficits and restores ERK signaling in the rat prefrontal cortex. Iran J Basic Med Sci 21, 1316–1321. https://doi.org/10.22038/IJBMS.2018.35368.8427

Sajikumar, S., Navakkode, S., Frey, J.U., 2007. Identification of compartment- and process-specific molecules required for “synaptic tagging” during long-term potentiation and long-term depression in hippocampal CA1. J. Neurosci. 27, 5068–5080. https://doi.org/10.1523/JNEUROSCI.4940-06.2007

Scharf, M.T., Woo, N.H., Lattal, K.M., Young, J.Z., Nguyen, P.V., Abel, T., 2002. Protein Synthesis Is Required for the Enhancement of Long-Term Potentiation and Long-Term Memory by Spaced Training. Journal of Neurophysiology 87, 2770–2777. https://doi.org/10.1152/jn.2002.87.6.2770

Schmitt, J.M., Stork, P.J.S., 2002. Gα and Gβγ Require Distinct Src-dependent Pathways to Activate Rap1 and Ras. Journal of Biological Chemistry 277, 43024–43032. https://doi.org/10.1074/jbc.M204006200

Schrader, L.A., Birnbaum, S.G., Nadin, B.M., Ren, Y., Bui, D., Anderson, A.E., Sweatt, J.D., 2006. ERK/MAPK regulates the Kv4.2 potassium channel by direct phosphorylation of the pore-forming subunit. American Journal of Physiology-Cell Physiology 290, C852–C861. https://doi.org/10.1152/ajpcell.00358.2005

Selcher, J.C., Atkins, C.M., Trzaskos, J.M., Paylor, R., Sweatt, J.D., 1999. A Necessity for MAP Kinase Activation in Mammalian Spatial Learning. Learn. Mem. 6, 478–490. https://doi.org/10.1101/lm.6.5.478

Selcher, J.C., Weeber, E.J., Christian, J., Nekrasova, T., Landreth, G.E., Sweatt, J.D., 2003. A Role for ERK MAP Kinase in Physiologic Temporal Integration in Hippocampal Area CA1. Learn. Mem. 10, 26–39. https://doi.org/10.1101/lm.51103

Shalin, S.C., Hernandez, C.M., Dougherty, M.K., Morrison, D.K., Sweatt, J.D., 2006. Kinase Suppressor of Ras1 Compartmentalizes Hippocampal Signal Transduction and Subserves Synaptic Plasticity and Memory Formation. Neuron 50, 765–779. https://doi.org/10.1016/j.neuron.2006.04.029

Singh, D., Bhalla, U.S., 2018. Subunit exchange enhances information retention by CaMKII in dendritic spines. Elife 7, 22. https://doi.org/10.7554/eLife.41412.001

Sweatt, J.D., 2004. Mitogen-activated protein kinases in synaptic plasticity and memory. Current Opinion in Neurobiology 14, 311–317. https://doi.org/10.1016/j.conb.2004.04.001

Sweatt, J.D., 1999. Toward a Molecular Explanation for Long-Term Potentiation. Learn. Mem. 6, 399–416. https://doi.org/10.1101/lm.6.5.399

Tang, S., Yasuda, R., 2017. Imaging ERK and PKA Activation in Single Dendritic Spines during Structural Plasticity. Neuron 93, 1315-1324.e3. https://doi.org/10.1016/j.neuron.2017.02.032

Terrell, E.M., Morrison, D.K., 2019. Ras-Mediated Activation of the Raf Family Kinases. Cold Spring Harbor Perspectives in Medicine 9. https://doi.org/10.1101/cshperspect.a033746

Walkup IV, W.G., Washburn, L., Sweredoski, M.J., Carlisle, H.J., Graham, R.L., Hess, S., Kennedy, M.B., 2015. Phosphorylation of Synaptic GTPase-activating Protein (synGAP) by Ca^{2+} /Calmodulin-dependent Protein Kinase II (CaMKII) and Cyclin-dependent Kinase 5 (CDK5) Alters the Ratio of Its GAP Activity toward Ras and Rap GTPases. Journal of Biological Chemistry 290, 4908–4927. https://doi.org/10.1074/jbc.M114.614420

Winder, D.G., Martin, K.C., Muzzio, I.A., Rohrer, D., Chruscinski, A., Kobilka, B., Kandel, E.R., 1999. ERK Plays a Regulatory Role in Induction of LTP by Theta Frequency Stimulation and Its Modulation by β-Adrenergic Receptors. Neuron 24, 715–726. https://doi.org/10.1016/S0896-6273(00)81124-1

Woo, N.H., Duffy, S.N., Abel, T., Nguyen, P.V., 2003. Temporal spacing of synaptic stimulation critically modulates the dependence of LTP on cyclic AMP-dependent protein kinase. Hippocampus 13, 293–300. https://doi.org/10.1002/hipo.10086

Young, J.Z., Isiegas, C., Abel, T., Nguyen, P.V., 2006. Metaplasticity of the late-phase of long-term potentiation: a critical role for protein kinase A in synaptic tagging. Eur J Neurosci 23, 1784–1794. https://doi.org/10.1111/j.1460-9568.2006.04707.x

Zhu, J.J., Qin, Y., Zhao, M., Van Aelst, L., Malinow, R., 2002. Ras and Rap Control AMPA Receptor Trafficking during Synaptic Plasticity. Cell 110, 443–455. https://doi.org/10.1016/S0092-8674(02)00897-8